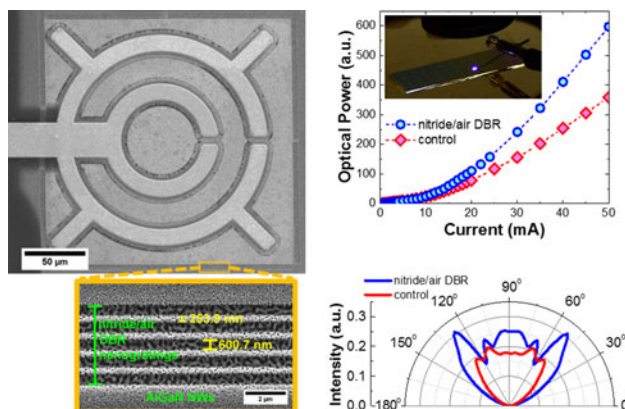


Enhancing the Light-Extraction Efficiency of an AlGaN Nanowire Ultraviolet Light-Emitting Diode by Using Nitride/Air Distributed Bragg Reflector Nanogratings

Volume 9, Number 5, October 2017

Mohd Sharizal Alias
Bilal Janjua
Chao Zhao
Davide Priante
Abdullah A. Alhamoud
Malleswararao Tangi
Lafi M. Alanazi
Abdullah A. Alatawi
Abdulrahman M. Albadri
Ahmed Y. Alyamani
Tien Khee Ng, *Member, IEEE*
Boon S. Ooi, *Senior Member, IEEE*



DOI: 10.1109/JPHOT.2017.2749198
1943-0655 © 2017 IEEE

Enhancing the Light-Extraction Efficiency of an AlGaIn Nanowire Ultraviolet Light-Emitting Diode by Using Nitride/Air Distributed Bragg Reflector Nanogratings

Mohd Sharizal Alias,¹ Bilal Janjua,¹ Chao Zhao,¹ Davide Priante,¹
Abdullah A. Alhamoud,¹ Malleswararao Tangi,¹ Lafi M. Alanazi,²
Abdullah A. Alatawi,¹ Abdulrahman M. Albadri,²
Ahmed Y. Alyamani,² Tien Khee Ng,¹ *Member, IEEE*,
and Boon S. Ooi,¹ *Senior Member, IEEE*

¹Photonics Laboratory, Computer, Electrical and Mathematical Sciences and Engineering Division, King Abdullah University of Science and Technology, Thuwal 23955-6900, Saudi Arabia

²National Center for Nanotechnology, King Abdulaziz City for Science and Technology, Riyadh 11442-6086, Saudi Arabia

DOI:10.1109/JPHOT.2017.2749198

1943-0655 © 2017 IEEE. Translations and content mining are permitted for academic research only. Personal use is also permitted, but republication/redistribution requires IEEE permission. See http://www.ieee.org/publications_standards/publications/rights/index.html for more information.

Manuscript received August 10, 2017; revised August 29, 2017; accepted August 31, 2017. Date of publication September 11, 2017; date of current version September 20, 2017. This work was supported by the King Abdulaziz City for Science and Technology under Grant KACST TIC R2-FP-008 and by the King Abdullah University of Science and Technology baseline funding BAS/1/1614-01-01. Corresponding author: Boon S. Ooi (e-mail: boon.ooi@kaust.edu.sa).

Abstract: The performance and efficiency of AlGaIn ultraviolet light-emitting diodes have been limited by the extremely low light-extraction efficiency (LEE) due to the intrinsic material properties of AlGaIn. Here, to enhance the LEE of the device, we demonstrate an AlGaIn nanowire light-emitting diode (NW-LED) integrated with nitride/air distributed Bragg reflector (DBR) nanogratings. Compared to a control device (only mesa), the AlGaIn NW-LED with the nitride/air DBR nanogratings exhibits enhancement in the light output power and external quantum efficiency (EQE) by a factor of ~ 1.67 . The higher light output power and EQE are attributed mainly to the multiple reflectances laterally for the transverse magnetic (TM)-polarized light and scattering introduced by the nanogratings. To further understand the LEE enhancement, the electrical field distribution, extraction ratio, and polar pattern of the AlGaIn NW-LED with and without the nitride/air DBR nanogratings were analyzed using the finite-difference time-domain method. It was observed that the TM-field emission was confined and scattered upward, whereas the polar pattern was intensified for the AlGaIn NW-LED with the nanogratings. Our approach to enhance the LEE via the nitride/air DBR nanogratings can provide a promising route for increasing the efficiency of AlGaIn-based LEDs, also, to functioning as facet mirror for AlGaIn-based laser diodes.

Index Terms: AlGaIn, nanowires, LED, DBR gratings.

1. Introduction

AlGaIn-based light-emitting diodes (LEDs) are promising technology for ultraviolet (UV) to deep-ultraviolet (DUV) light source for applications such as solar-blind free-space communication, lithographic microfabrication, biochemical-sensing, air/water purification, surface/food sterilization,

UV curing, and medical diagnostics [1]. Several devices have shown external quantum efficiency (EQE) of 10–12% [1]–[3]. However, further improvement is required to realize the above applications. Basically, the EQE of a LED is the product of the internal quantum efficiency (IQE) and light-extraction efficiency (LEE) [1], [3], [4]. Both efficiencies are important to be optimized for obtaining AlGa_N LEDs with high EQE. While the IQE has been improved recently up to 60% by improving the crystalline quality [2], the LEE is still lacking (<10%) [1], [5], [6] due to the limitations such as high absorption of the p-GaN contact layer [7], anisotropic optical polarization properties of the AlGa_N material especially for high Al composition [8]–[10], low reflectivity of the metal contacts at the UV regime [11], [12], and high absorption of the encapsulation packaging material [2], [4].

Several efforts have been demonstrated to increase the LEE of AlGa_N LEDs using advanced light extraction techniques such as UV transparent contact layer [6], [13], [14], surface roughening/texturing [15]–[17], patterned sapphire substrate [18], [19], integrating micro-/hemispherical lenses on the sapphire substrate [4], [20], reflective metal electrodes [6], [12], [21], reflective scattering structure (RSS) [22], anti-reflective coating [23], nanowires/nanorods [24], [25], photonic crystals [26]–[28], surface plasmonics [29], sidewall emission enhancement (SEE) [30], [31], nanostructured AlN substrate [32], [33], micro/nano-pixel LEDs [12], [34], and encapsulation using UV transparent materials [2], [5], [6]. However, most of these techniques were less effective for the AlGa_N LEDs because it only enhanced the light-extraction for the transverse electric (TE)-polarized light. The uniqueness of the anisotropic optical polarization properties of the AlGa_N material allowed the light emission as either TE- or transverse magnetic (TM)-mode from the *c*-plane of the AlGa_N structure. The TE-mode (electrical field, $E_{\perp c}$ -axis) propagates in the out-of-plane direction whereas the TM-mode ($E_{\parallel c}$ -axis) propagates in the in-plane direction. The TM-mode starts to dominate in AlGa_N LED as the Al composition increased towards the DUV wavelengths [8]–[10]. As such, more TM-polarized light is trapped in the device laterally (the trapped light will eventually be absorbed) rather than being emitted out because the escape cone of the LED is typically in the out-of-plane direction. Among the light-extraction techniques mentioned above, only the SEE [30], [31], nanowires/nanorods [24], [25], micro/nano-pixel LEDs [12], [34], and the RSS [22], are considered attractive for AlGa_N LEDs because these techniques enhanced the emission of TM-polarized light. However, these techniques (except for the nanowires/nanorods) utilized Al metallic layer which is not perfectly reflective (85–92% reflectivity, R) at the UV wavelengths and not forming effective ohmic contacts with p-GaN contact layer [11], [12], [21]. Moreover, the reflectivity of the Al reduced significantly ($R < 20\%$) at the DUV wavelengths upon annealing [21]. Also, the SEE technique required the regrowth of GaN structure which further complicates the device processing [30]. Although AlGa_N-based nanowires/nanorods have shown to enhance the TM-polarized light [24], [25] by scattering effect, these nanostructures can also absorb more light due to the inhomogeneity.

Here, to enhance the LEE of the device, we demonstrate an AlGa_N nanowires light-emitting diode (NWs-LED) integrated with nitride/air Distributed Bragg Reflector (DBR) nanogratings. The DBR is a mirror structure composed of multiple periods of an alternating high- and low-refractive index (RI) layers, and can be designed to be highly reflective ($R > 99\%$). These DBR nanogratings were patterned using gas-assisted focused-ion beam (GAFIB) technique which acts as a reflector for the in-plane light propagation (TM-polarized light). We show that by having the nitride/air DBR nanogratings as the light-extractor, the light output power and EQE for the AlGa_N NWs-LED improved by a factor of ~ 1.67 . We also analyze theoretically the electric field distribution, extraction ratio and polar pattern of the device using the finite-difference-time-domain (FDTD) method.

2. Device Structure and Fabrication

The AlGa_N NWs were grown by plasma-assisted molecular beam epitaxy technique on a Si substrate. The growth details and the material characterizations are described elsewhere [35]. Briefly, from bottom-up, the NWs-LED epistructure were composed of a 100 nm thick GaN buffer layer, a 20 nm thick Si-doped n-Al_xGa_{1-x}N graded layers (with $x = 0.05$ to 0.20), a 75 nm thick Si-doped n-Al_{0.27}Ga_{0.73}N clad layer, an active region composed of 15 stacks of 1 nm thick Al_{0.11}Ga_{0.89}N quantum disks separated by 3.5 nm thick Al_{0.27}Ga_{0.73}N quantum barriers, a 20 nm thick Mg-doped

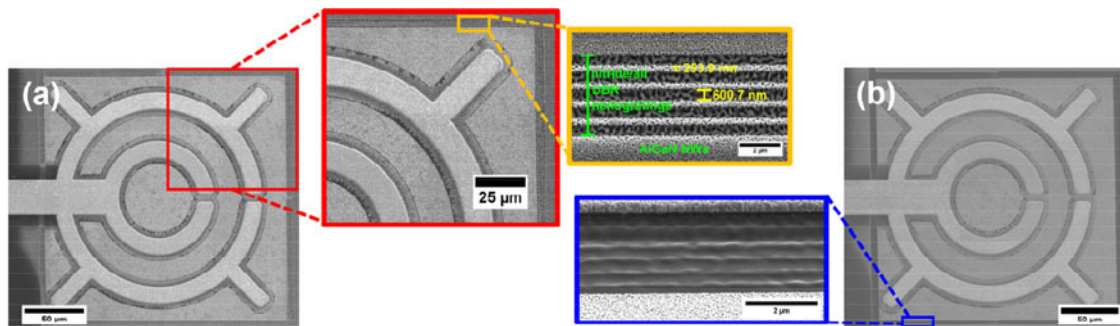


Fig. 1. The top-view SEM micrographs of the AlGa_N NWs-LED with (a) the nitride/air DBR nanogratings patterned at all edges of the device with inset showing the dimension of the nanogratings, and (b) only mesa formed for the control device (inset shows all nanogratings were etched, the image at perspective view (tilted 52°) for clarity).

p-Al_{0.35}Ga_{0.65}N clad layer, a 10 nm thick Mg-doped p-Al_xGa_{1-x}N graded layers (with $x = 0.05$ to 0.30), and a 30 nm thick Mg-doped p-GaN contact layer. The AlGa_N NWs-LEDs were fabricated using standard device processing as described in previous work [36]. Fig. 1(a) shows the top-view of the scanning electron microscope (SEM) micrograph of the fabricated AlGa_N NWs-LED (device size $200 \times 200 \mu\text{m}^2$) with the nitride/air DBR nanogratings (inset) patterned on all sides. After performing the device characterizations, the same device was etched by GAFIB etching to form a control device (with mesa only) as shown in Fig. 1(b). The nitride/air DBR nanogratings were etched completely as exhibited in the inset of Fig. 1(b). By using the same device for comparison, any argument on the NWs inhomogeneity is avoided.

3. DBR Nanogratings Patterning

To form the nitride/air DBR nanogratings, we determined the effective refractive index (n_{eff}) of the AlGa_N NWs using the spectroscopic ellipsometry (SE) technique. Since the wavelength of interest is within the UV regime, we used a phase modulated SE where the signals detected were in the form of harmonics that can be extracted to determine the ellipsometric angles as a function of energy [37]. Fig. 2(a) shows the wavelength-dependent n_{eff} spectra for the AlGa_N NWs, indicating n_{eff} of 2.371 at the emission wavelength of the LED which is ~ 343 nm. Although we used 343 nm wavelength UVLED, the TM-polarization still exist strongly, i.e., 40–60% within the wavelength range of 320–350 nm [8]–[10]. Furthermore, our approach of using the nitride/air DBR nanogratings applies to any shorter wavelength AlGa_N-based UV-LED. For validation of the measured n_{eff} , we performed a theoretical calculation using the effective index method (EIM) and obtained a value of 2.384 (Fig. 2(b)). The measured n_{eff} is slightly lower due to the existence of air-voids in between the AlGa_N NWs. To obtain a quality etching profile for the nanogratings by controlling the etching aspect ratio to less than two, the DBR was designed as seventh-order gratings. Using the SE measured index, the widths (thickness) of the nitride and air corresponding to $7\lambda/4n_{\text{eff}} = 253.16$ nm and $7\lambda/4n_{\text{air}} = 600.25$ nm, respectively, with $\lambda = 343$ nm. From the transfer matrix method (TMM) calculation, using five pairs of the nitride/air DBR nanogratings, we obtained a $R \sim 99.9\%$ reflector as shown in Fig. 2(c). The DBR stopband ($R > 90\%$) is ~ 30 nm with the electroluminescence (EL) spectra of the AlGa_N NWs-LED located centrally (Fig. 2(c)). We then patterned the nitride/air DBR nanogratings at all device edges using the GAFIB etching with I₂ halide gaseous precursor. We demonstrated a high uniformity and periodicity of nanogratings patterning with nanoscale precision as shown in the SEM micrographs (Fig. 2(d)). Although the FIB etching throughput can be considered low, by using the chemical-assisted etching, the etch-rate for nitride material is enhanced by a factor of nine [38]. Recently, we have shown that the GAFIB technique can be used to pattern nanoscale structure with high uniformity and precision even for

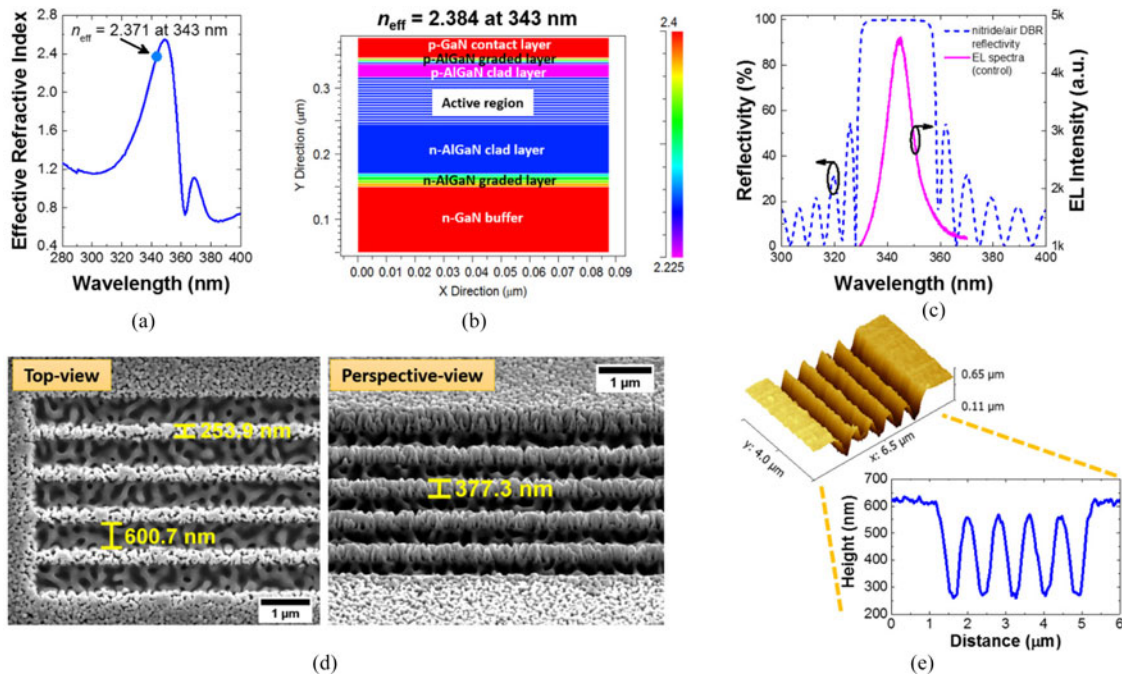


Fig. 2. (a) The n_{eff} as a function of wavelength for the AlGaIn NWs as measured by SE technique. (b) Calculated n_{eff} for the AlGaIn NWs structure. (c) The calculated reflectivity of the nitride/air DBR nanogratings and measured EL as a function of wavelength. (d) SEM micrographs of the patterned nitride/air DBR nanogratings from top-view and perspective-view (tilted 52°). (e) 3-D topography and the line-scan (inset) of the nitride/air DBR nanogratings as measured by AFM technique.

a material with air-voids such as hybrid perovskites [39], [40] (similarity here where air-voids exist in between AlGaIn NWs). Fig. 2(e) shows the 3D topography of the nitride/air DBR nanogratings measured using the atomic force microscopy (AFM), with the etch-depth ~ 340 nm as indicated by the AFM line-scan (inset). The patterned nanogratings exhibit sidewall angle of ~ 83 – 85° , which can result in lower reflectivity than the calculated $R = 99.9\%$ from the TMM calculation that assumed a vertical sidewall (angle of 90°). It has been reported that the reflectivity reduced from 90% to 70% for a fifth-order nitride/air DBR gratings (at $\lambda = 400$ nm) with a sidewall angle of 85° [41]. Nevertheless, the reflectivity obtained by the nitride/air DBR nanogratings is still high compared to only nitride-air interface which is typically $\sim 17\%$ reflective [42], [43].

4. Device Characteristics

For the device characteristics, the details of the experiment are described in our earlier work [35], [36]. The EL spectra for the device with nitride/air DBR nanogratings and without nanogratings (control device) are shown in Fig. 3(a) and (b), respectively. The AlGaIn NWs-LED with the nanogratings exhibits stronger EL emission intensity by a factor of ~ 1.69 (at 50 mA injected current) compared to the control device. As for the full-width-of-half-maximum (FWHM) from the EL spectra of the AlGaIn NWs-LED with the nanogratings, the FWHM narrowed quickly reaching ~ 12 nm as the injected current increased (Fig. 3(c)). In comparison, the FWHM of the control device narrowed slowly and only demonstrated FWHM of ~ 15 nm. Both EL spectra and FWHM results indicated that the light was emitted with higher intensity and exhibited a degree of light confinement when the nitride/air DBR nanogratings were integrated on the AlGaIn NWs-LED.

Fig. 3(d)–(f) show the comparison of the light output power-current (L - I) curve, current-voltage (I - V) curve, and the normalized EQE, respectively, between the AlGaIn NWs-LED with the nitride/air DBR nanogratings and the control device. The devices were only biased from 0 to 50 mA and 0

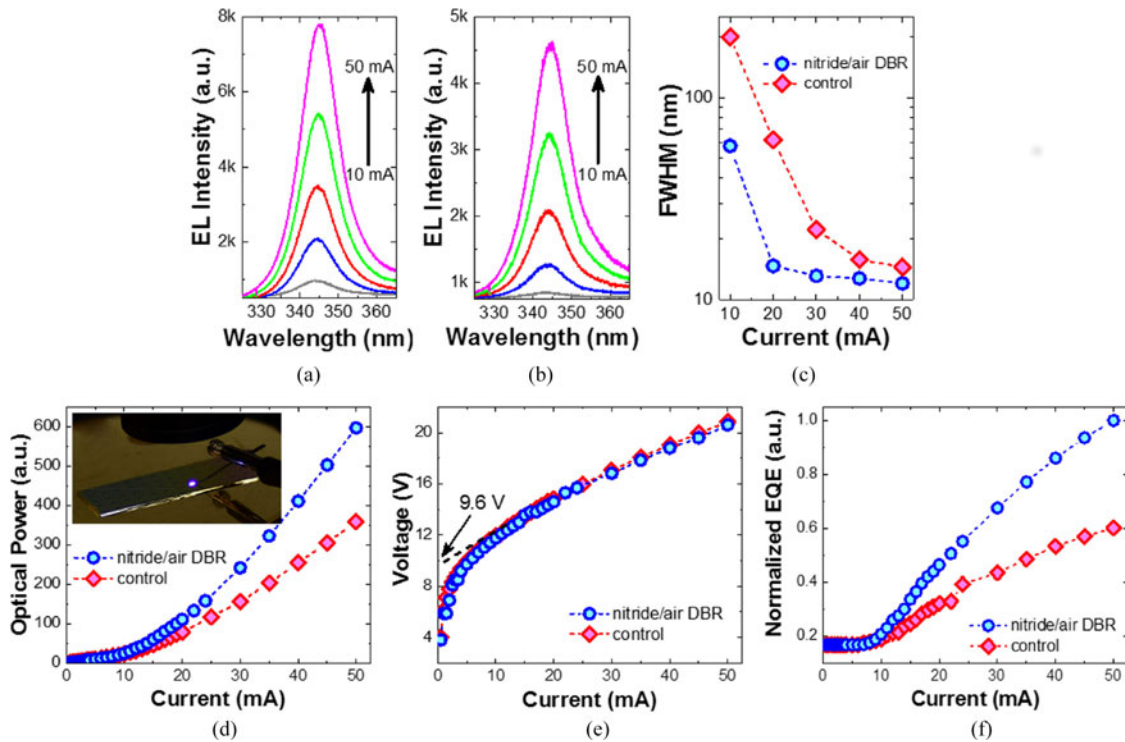


Fig. 3. The device characteristics comparison between the AlGaIn NWs-LED with nitride/air DBR nanogratings and control device showing (a) EL spectra for the device with nanogratings, (b) EL spectra for the control device with mesa only, (c) FWHM plot (semi-log scale) as the injection current increased, (d) L - I curve (device with nanogratings under electrical probed inset), (e) I - V curve, and (f) device EQE. The dashed lines are added to guide the eye.

to 20 V for the L - I and I - V curves, respectively, to avoid device breakdown since the same device was completely etched later to function as the control device. The AlGaIn NWs-LED with the nanogratings emitted higher light output power compared to the control device (Fig. 3(d)) above 15 mA injected current onwards. At an injected current of 50 mA (inset of Fig. 3(d) shows the device under electrical probing), the enhancement is by a factor of ~ 1.67 . For comparison, enhancement of light output power for improvement factors up to ~ 1.35 and ~ 1.61 were reported for AlGaIn LEDs utilizing SEE [31] and nano-pixel [12] as the in-plane light-extraction techniques. The similarity in term of the trend for the I - V curve and the turn-on voltage (Fig. 3(e)) indicate that the GAFIB etching does not introduce any significant surface damage or layer amorphization during the nanogratings patterning. The turn-on voltage for both devices (~ 9.6 V) was consistent with our previous grown device on Si substrate [36]. Higher EQE was obtained for the device with the nanogratings (Fig. 3(f)), resulted from the improvement of the LEE of the device. The enhancement of the light output power and EQE for the AlGaIn NWs-LED with nitride/air DBR nanogratings can be attributed to two factors. First, the in-plane light emission (TM-mode) is experiencing multiple reflections from the nanogratings laterally. The back reflected light then coupled with the out-of-plane emission, thus enhancing the LEE of the device. The second factor is the non-vertical sidewall angle of the nanogratings (as shown in Fig. 2(e) from the AFM measurements) which typically occurs in etching process also helped to scatter the light towards the out-of-plane emission. To ensure the consistency and reliability of our results, we fabricated additional devices with the same device dimension. The device measurements show consistency for the enhancement of the light output power from ~ 1.59 to 1.64.

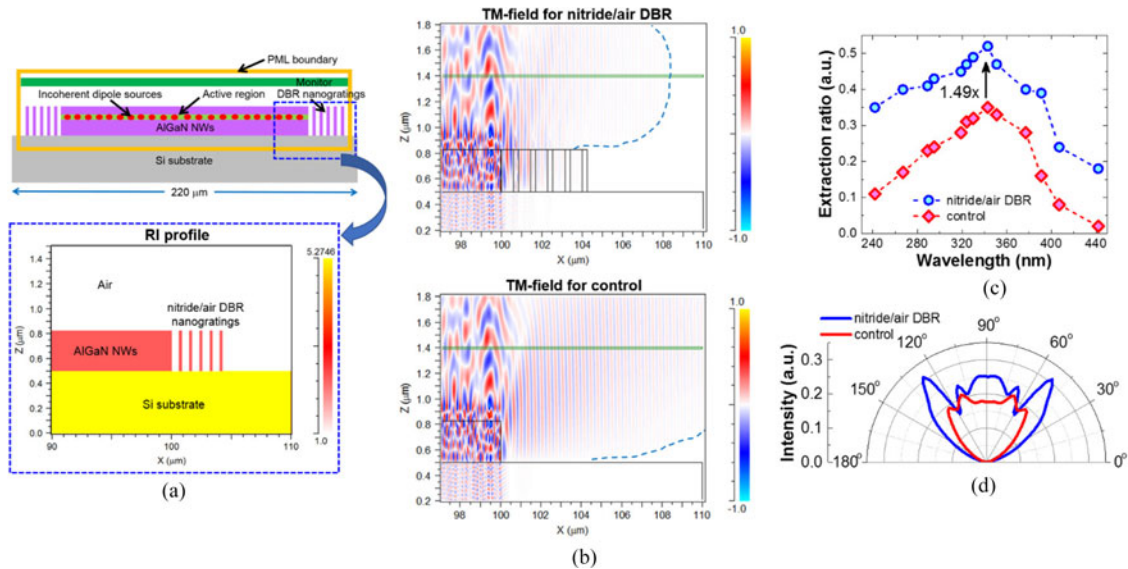


Fig. 4. (a) Schematic of the FDTD analysis of the AlGaIn NWs-LED, here showing the device with nitride/air DBR nanogratings case with the RI profile inset. (b) Calculated electric field distribution of the TM-mode for device with and without the nanogratings, the dashed lines are added to indicate the light scattering. The solid black and green lines indicate the device structure and the surface monitor. (c) Calculated extraction ratio for both devices, the dashed lines are added to guide the eye. (d) Comparison of the calculated polar pattern for both devices.

5. FDTD Simulation and Analysis

To further investigate the device analysis, we performed the FDTD calculation for the electric field distribution, extraction ratio, and polar pattern. Briefly, the FDTD calculates the differential forms of Maxwell's equations using specific boundary conditions for a given structure to obtain rigorous solutions for the electromagnetic wave propagation. Further details of this numerical method can be found in [44] and recent example of an application for AlGaIn NWs can be referred in [45]. The schematic of FDTD modeling for our device is shown in Fig. 4(a) with the inset displays the RI profile with the nanogratings at one end. The RI for the AlGaIn NWs and Si substrate were set as 2.371 and 5.275, respectively. We used ~ 1150 dipole sources (emission wavelength and FWHM were set at 343 nm and 12 nm, correspondingly) across the active region layer to mimic the NWs (diameter of NW is ~ 175 – 200 nm). These dipole sources were set with spatially incoherent unpolarized conditions, where the simulated radiation properties were averaged from three orthogonal orientations for each dipole to mimic the spontaneous emission of LED. The simulation domain is set as $220 \mu\text{m} \times 1.5 \mu\text{m}$ with the non-uniform mesh being applied (the grid size was 10 nm in the bulk and 3 nm at the interface). The simulation domain was enclosed with perfectly matched layer (PML) boundary to absorb outgoing light without being reflected. Two monitors were used, i.e., surrounding the dipole sources to measure the electric field radiated, and on the surface (at λ distance) to measure the far-field generated, respectively. Fig. 4(b) shows the electric field distribution of the TM-mode. It shows that the nitride/air DBR nanogratings reflected most of the in-plane light emission and even introduced scattering effect for a vertical sidewall nanogratings. It has been shown that $\sim 3.5\%$ of the propagated light is being scattered upward for a vertical sidewall fifth-order InP-based/air DBR gratings [46]. As for the control device, the in-plane light emission only continues to propagate laterally. A theoretical extraction ratio (defined as the ratio of the emitted power from the surface to the emitted power from the active region) can be determined at the device surface. We found that the extraction ratio for the AlGaIn NWs-LED with nitride/air DBR nanogratings increased by a factor of 1.49 at the wavelength of 343 nm compared to the control device (Fig. 4(c)). This value is within the experiment which is around 1.42 to 1.67

depending on the injected current bias. Fig. 4(d) exhibits the calculated polar pattern (with 90° as the normal to the emission surface) for the AlGaIn NWs-LED with nitride/air DBR nanogratings and the control device. The device with the nanogratings demonstrated enhancement and narrowing of the out-of-plane emission. It also exhibits improvement factor of ~ 1.44 for the far-field (FF) intensity. Sideway angle emissions are pointing at approximately 50 and 130° also appeared due to the light being scattered from the nitride/air DBR nanogratings. Thus, the integration of nitride/air DBR nanogratings with the AlGaIn NWs-LED indicates an enhancement in FF intensity and radiance.

6. Conclusion

In summary, an enhancement of LEE for AlGaIn NWs-LED was demonstrated by integrating nitride/air DBR nanogratings at the edges of the device. The nanogratings were patterned with high uniformity and precision using the GAFIB technique. We observed an enhancement of light output power and the EQE by a factor of ~ 1.67 compared to the control device. By implementing the nitride/air DBR nanogratings, the TM-field emission, extraction ratio and polar pattern of the AlGaIn NWs-LED improved as discussed in the FDTD analysis. These device improvements were attributed mainly to the multiple reflectances laterally for the TM-polarized light and scattering introduced by the nanogratings. Besides improving the efficiencies (LEE and EQE) of the AlGaIn LED, the nitride/air DBR nanogratings can also be applied to the facet of AlGaIn based laser diodes to improve the device performance.

References

- [1] M. Kneissl and J. Rass, *III-Nitride Ultraviolet Emitters: Technology and Applications*. Switzerland: Springer, 2016.
- [2] M. Shatalov *et al.*, "AlGaIn deep-ultraviolet light-emitting diodes with external quantum efficiency above 10%," *Appl. Phys. Express*, vol. 5, no. 8, Jul. 2012, Art. no. 082101.
- [3] M. Shatalov *et al.*, "High power AlGaIn ultraviolet light emitters," *Semicond. Sci. Technol.*, vol. 29, no. 8, Jun. 2014, Art. no. 084007.
- [4] M. Ichikawa *et al.*, "High-output-power deep ultraviolet light-emitting diode assembly using direct bonding," *Appl. Phys. Express*, vol. 9, no. 7, Jun. 2016 Art. no. 072101.
- [5] K. Yamada *et al.*, "Development of underfilling and encapsulation for deep-ultraviolet LEDs," *Appl. Phys. Express*, vol. 8, no. 1, Jan. 2015, Art. no. 012101.
- [6] T. Takano, T. Mino, J. Sakai, N. Noguchi, K. Tsubaki, and H. Hirayama, "Deep-ultraviolet light-emitting diodes with external quantum efficiency higher than 20% at 275 nm achieved by improving light-extraction efficiency," *Appl. Phys. Express*, vol. 10, no. 3, Feb. 2017, Art. no. 031002.
- [7] J. F. Muth *et al.*, "Absorption coefficient, energy gap, exciton binding energy, and recombination lifetime of GaN obtained from transmission measurements," *Appl. Phys. Lett.*, vol. 71, no. 18, pp. 2572–2574, 1997.
- [8] J. Shakya, K. Knabe, K. H. Kim, J. Li, J. Y. Lin, and H. X. Jiang, "Polarization of III-nitride blue and ultraviolet light-emitting diodes," *Appl. Phys. Lett.*, vol. 86, no. 9, 2005, Art. no. 091107.
- [9] T. Kolbe *et al.*, "Optical polarization characteristics of ultraviolet (In)(Al)GaIn multiple quantum well light emitting diodes," *Appl. Phys. Lett.*, vol. 97, no. 17, 2010, Art. no. 171105.
- [10] K. B. Nam, J. Li, M. L. Nakarmi, J. Y. Lin, and H. X. Jiang, "Unique optical properties of AlGaIn alloys and related ultraviolet emitters," *Appl. Phys. Lett.*, vol. 84, no. 25, pp. 5264–5266, 2004.
- [11] J. K. Kim *et al.*, "Enhanced light-extraction in GaInN near-ultraviolet light-emitting diode with Al-based omnidirectional reflector having NiZn/Ag microcontacts," *Appl. Phys. Lett.*, vol. 89, no. 14, 2006, Art. no. 141123.
- [12] N. Lobo *et al.*, "Enhancement of light extraction in ultraviolet light-emitting diodes using nanopixel contact design with Al reflector," *Appl. Phys. Lett.*, vol. 96, no. 8, 2010, Art. no. 081109.
- [13] N. Maeda and H. Hirayama, "Realization of high-efficiency deep-UV LEDs using transparent p-AlGaIn contact layer," *Phys. Status Solidi Current Topics Solid State Phys.*, vol. 10, no. 11, pp. 1521–1524, 2013.
- [14] M. Jo, N. Maeda, and H. Hirayama, "Enhanced light extraction in 260 nm light-emitting diode with a highly transparent p-AlGaIn layer," *Appl. Phys. Express*, vol. 9, no. 1, Jan. 2016, Art. no. 012102.
- [15] B. J. Kim *et al.*, "Enhancement of light extraction efficiency of ultraviolet light emitting diodes by patterning of SiO₂ nanosphere arrays," *Thin Solid Films*, vol. 517, no. 8, pp. 2742–2744, 2009.
- [16] L. Zhou *et al.*, "Vertical injection thin-film AlGaIn/AlGaIn multiple-quantum-well deep ultraviolet light-emitting diodes," *Appl. Phys. Lett.*, vol. 89, no. 24, 2006, Art. no. 241113.
- [17] C. E. Lee, B. S. Cheng, Y. C. Lee, H. C. Kuo, T. C. Lu, and S. C. Wang, "Output power enhancement of vertical-injection ultraviolet light-emitting diodes by GaN-free and surface roughness structures," *Electrochem. Solid-State Lett.*, vol. 12, no. 2, pp. H44–H46, 2009.
- [18] M. Kim *et al.*, "AlGaIn-based deep ultraviolet light-emitting diodes fabricated on patterned Sapphire substrates," *Appl. Phys. Exp.*, vol. 4, no. 9, Aug. 2011, Art. no. 092102.

- [19] P. Dong *et al.*, “282-nm AlGaIn-based deep ultraviolet light-emitting diodes with improved performance on nano-patterned sapphire substrates,” *Appl. Phys. Lett.*, vol. 102, no. 24, Jun. 2013, Art. no. 241113.
- [20] M. Khizar, Z. Y. Fan, K. H. Kim, J. Y. Lin, and H. X. Jiang, “Nitride deep-ultraviolet light-emitting diodes with microlens array,” *Appl. Phys. Lett.*, vol. 86, no. 17, 2005, Art. no. 173504.
- [21] T. Inazu *et al.*, “Improvement of light extraction efficiency for AlGaIn-based deep ultraviolet light-emitting diodes,” *Jpn. J. Appl. Phys.*, vol. 50, no. 12R, Nov. 2011, Art. no. 122101.
- [22] J. J. Wierer, A. A. Allerman, I. Montaño, and M. W. Moseley, “Influence of optical polarization on the improvement of light extraction efficiency from reflective scattering structures in AlGaIn ultraviolet light-emitting diodes,” *Appl. Phys. Lett.*, vol. 105, no. 2, 2005, Art. no. 061106.
- [23] X. Yan, M. Shatalov, T. Saxena, and M. S. Shur, “Deep-ultraviolet tailored- and low-refractive index antireflection coatings for light-extraction enhancement of light emitting diodes,” *J. Appl. Phys.*, vol. 113, no. 16, 2013, Art. no. 163105.
- [24] M. Djavid and Z. Mi, “Enhancing the light extraction efficiency of AlGaIn deep ultraviolet light emitting diodes by using nanowire structures,” *Appl. Phys. Lett.*, vol. 108, no. 5, 2016, Art. no. 051102.
- [25] H.-Y. Ryu, “Large enhancement of light extraction efficiency in AlGaIn-based nanorod ultraviolet light-emitting diode structures,” *Nanoscale Res. Lett.*, vol. 9, no. 1, 2014, Art. no. 58.
- [26] T. N. Oder, K. H. Kim, J. Y. Lin, and H. X. Jiang, “III-nitride blue and ultraviolet photonic crystal light emitting diodes,” *Appl. Phys. Lett.*, vol. 84, no. 4, pp. 466–468, 2004.
- [27] J. Shakya, K. H. Kim, J. Y. Lin, and H. X. Jiang, “Enhanced light extraction in III-nitride ultraviolet photonic crystal light-emitting diodes,” *Appl. Phys. Lett.*, vol. 85, no. 1, pp. 142–144, 2004.
- [28] M. S. Alias, S. Shaari, P. O. Leisher, and K. D. Choquette, “Highly confined and continuous single-mode operation of self-align photonic crystal oxide VCSEL,” *Appl. Phys. B*, vol. 100, no. 3, pp. 453–459, 2010.
- [29] N. Gao, K. Huang, J. Li, S. Li, X. Yang, and J. Kang, “Surface-plasmon-enhanced deep-UV light emitting diodes based on AlGaIn multi-quantum wells,” *Sci. Rep.*, vol. 2, 2012, Art. no. 816.
- [30] D. Y. Kim *et al.*, “Overcoming the fundamental light-extraction efficiency limitations of deep ultraviolet light-emitting diodes by utilizing transverse-magnetic-dominant emission,” *Light Sci. Appl.*, vol. 4, 2015, Art. no. e263.
- [31] J. W. Lee *et al.*, “An elegant route to overcome fundamentally-limited light extraction in AlGaIn deep-ultraviolet light-emitting diodes: Preferential outcoupling of strong in-plane emission,” *Sci. Rep.*, vol. 6, 2016, Art. no. 22537.
- [32] S.-i. Inoue, T. Naoki, T. Kinoshita, T. Obata, and H. Yanagi, “Light extraction enhancement of 265 nm deep-ultraviolet light-emitting diodes with over 90 mW output power via an AlN hybrid nanostructure,” *Appl. Phys. Lett.*, vol. 106, no. 13, 2015, Art. no. 131104.
- [33] S.-i. Inoue, N. Tamari, and M. Taniguchi, “150 mW deep-ultraviolet light-emitting diodes with large-area AlN nanophotonic light-extraction structure emitting at 265 nm,” *Appl. Phys. Lett.*, vol. 110, no. 14, 2017, Art. no. 141106.
- [34] W. Shuai, A. Vinod, S. Maxim, C. Ashay, S. Wen-Hong, and M. A. Khan, “Micro-pixel design milliwatt power 254 nm Emission Light Emitting Diodes,” *Jpn. J. Appl. Phys.*, vol. 43, no. 8A, pp. L1035–L1037, 2004.
- [35] B. Janjua *et al.*, “Droop-free $\text{Al}_x\text{Ga}_{1-x}\text{N}/\text{Al}_y\text{Ga}_{1-y}\text{N}$ quantum-disks-in-nanowires ultraviolet LED emitting at 337 nm on metal/silicon substrates,” *Opt. Exp.*, vol. 25, no. 2, pp. 1381–1390, 2017.
- [36] B. Janjua *et al.*, “Self-planarized quantum-disks-in-nanowires ultraviolet-B emitters utilizing pendeo-epitaxy,” *Nanoscale*, vol. 9, pp. 7805–7813, 2017.
- [37] M. S. Alias *et al.*, “Optical constants of $\text{CH}_3\text{NH}_3\text{PbBr}_3$ perovskite thin films measured by spectroscopic ellipsometry,” *Opt. Exp.*, vol. 24, no. 15, pp. 16586–16594, 2016.
- [38] I. Chyr and A. J. Steckl, “GaIn focused ion beam micromachining with gas-assisted etching,” *J. Vacuum Sci. Technol. B*, vol. 19, no. 6, pp. 2547–2550, 2001.
- [39] M. S. Alias *et al.*, “Focused-ion beam patterning of organolead trihalide perovskite for subwavelength grating nanophotonic applications,” *J. Vacuum Sci. Technol. B*, vol. 33, no. 5, 2015, Art. no. 051207.
- [40] M. S. Alias *et al.*, “Enhanced etching, surface damage recovery, and submicron patterning of hybrid perovskites using a chemically gas-assisted focused-ion beam for subwavelength grating photonic applications,” *J. Phys. Chem. Lett.*, vol. 7, no. 1, pp. 137–142, 2016.
- [41] H. L. Wang, T. Tawara, M. Kumagai, T. Saftoh, and N. Kobayashi, “Novel design to fabricate high reflectivity GaIn-based semiconductor/air distributed Bragg reflector with the tilt of vertical sidewall,” *Jpn. J. Appl. Phys.*, vol. 41, no. 6B, pp. L682–L684, 2002.
- [42] T. Kotani *et al.*, “Fabrication and characterization of GaIn-based distributed Bragg reflector mirrors for low lasing threshold and integrated photonics,” *Phys. Status Solidi Current Topics Solid State Phys.*, vol. 2, no. 7, pp. 2895–2898, 2005.
- [43] H. Wang *et al.*, “Fabrication of an InGaIn multiple-quantum-well laser diode featuring high reflectivity semiconductor/air distributed Bragg reflectors,” *Appl. Phys. Lett.*, vol. 81, no. 25, pp. 4703–4705, 2002.
- [44] A. Taflove and S. C. Hagness, *Computational Electrodynamics: The Finite-Difference Time-Domain Method*. Norwood, MA, USA: Artech House, 2005.
- [45] Y. K. Ooi, C. Liu, and J. Zhang, “Analysis of polarization-dependent light extraction and effect of passivation layer for 230-nm AlGaIn nanowire light-emitting diodes,” *IEEE Photon. J.*, vol. 9, no. 4, Aug. 2017, Art. no. 4501712.
- [46] M. Ariga *et al.*, “Low threshold GaInAsP lasers with semiconductor/air distributed Bragg reflector fabricated by inductively coupled plasma etching,” *Jpn. J. Appl. Phys.*, vol. 39, no. 6A, pp. 3406–3409, 2000.